$^{16}O(^{7}Li,^{7}Be)^{16}N$ reaction at 50 MeV

J. Cook and K. W. Kemper
Department of Physics, Florida State University, Tallahassee, Florida 32306

P. V. Drumm, L. K. Fifield, M. A. C. Hotchkis, T. R. Ophel, and C. L. Woods
Department of Nuclear Physics, Institute of Advanced Studies, The Australian National University, Canberra, ACT 2600, Australia

(Received 19 June 1984)

The elastic scattering of $^{7}Li+^{16}O$ has been measured at $E_{Li}=50$ MeV and fitted with an optical model potential. The $^{16}O(^{7}Li,^{7}Be)^{16}N$ reaction has been investigated at $E_{Li}=50$ MeV. States and groups of states were observed up to 6.3 MeV excitation in the $^{16}N+^{7}Be$ system. Angular distributions for ^{16}N in 2^- 0.0 MeV, 3^- 0.297 MeV, and 4^- 6.17 MeV states with ^{7}Be in its ground state ($^{7}Be_0$), and for ^{16}N in the 3^- 0.297 MeV state with ^{7}Be in its first excited state ($^{7}Be_1$), have been compared with distorted-wave Born approximation calculations. The distorted-wave Born approximation form factors were calculated microscopically using central and tensor forces and realistic transition densities. The calculations fail to reproduce the cross sections.

I. INTRODUCTION

The question as to whether charge exchange reactions involving composite particles proceed by a simple one-step process, or by complicated multistep routes, is still unresolved. The difficulty in interpreting the analysis of the experiments is that there is no clear signature of success or failure. In general, the interaction strengths are treated as free parameters and adjusted to describe the data. Previous studies[1,2] of the ($^{7}Li,^{7}Be$) reaction leading to states in ^{28}Al and ^{40}K seemed to be consistent with a one-step interpretation because the interaction strengths were reasonable. However, one important test of these interactions that could not be made, because of the limited energy resolution, was a determination of the relative strengths of the central and tensor components. It is necessary to experimentally resolve the natural and unnatural parity states to be able to do this because the former is dominated by the central force and the latter by the tensor force. These states were not resolved in the previously published ($^{7}Li,^{7}Be$) studies.

In the present work, the $^{16}O(^{7}Li,^{7}Be)^{16}N$ reaction is studied. The states in ^{16}N are sufficiently well separated that the natural and unnatural parity states can be experimentally resolved. The low-lying four states in ^{16}N are well described[3] by the $d_{5/2}p_{1/2}^{-1}$ or $s_{1/2}p_{1/2}^{-1}$ configurations. The lack of any other states below 3 MeV in ^{16}N decreases the amount of configuration mixing in these states. The $^{17}O(d,^{3}He)^{16}N$ reaction[4] has spectroscopic factors of about unity for the 2^- 0.0 MeV and 3^- 0.297 MeV states, thus confirming their dominant one-particle—one-hole (1p1h) character. In addition, the pickup reaction suggests a stretched $d_{5/2}p_{3/2}^{-1}$ configuration for the 4^- 6.17 MeV state. The ($d,^{3}He$) transfer data were measured simultaneously with that for $^{17}O(d,t)$ so that clear analog assignments could be made to the 2^- 12.969 MeV, 3^- 13.254 MeV, and 4^- 18.97 MeV $T=1$ states in ^{16}O. These states are predicted[5] to have less than 9% 3p3h admixtures. The assignment of 4^- and a relatively pure 1p1h excitation to the 18.97 MeV state in ^{16}O has been confirmed by medium energy inelastic proton,[6] pion,[7] and electron[8] scattering measurements in addition to $^{13}C(^{6}Li,t)$ results.[9] The previously discussed 1p1h states in ^{16}N should then be good candidates for charge exchange reaction studies.

In the present work, angular distributions at $E(^{7}Li)=50$ MeV were taken for the $^{16}O(^{7}Li,^{7}Be)^{16}N$ reaction as well as $^{7}Li+^{16}O$ elastic scattering. The heavy-ion detection system used was able to resolve the low-lying states populated in ^{16}N. A microscopic interaction was used in distorted wave calculations which were compared with the data.

II. EXPERIMENTAL METHOD

Beams of ^{7}Li at 50 MeV were obtained from the Australian National University (ANU) 14 UD Pelletron tandem accelerator. The targets were natural SiO_2 on an Au backing and contained about 70 $\mu g\,cm^{-2}$ of oxygen. The target thicknesses were found by scattering 1.8 MeV protons into a detector of known solid angle at a laboratory angle of 150° and then comparing the elastic yields to previously reported[10] cross sections. The low energy protons were obtained from an auxiliary ANU Van de Graaff accelerator. The error in the absolute cross section is $\pm 15\%$ and arises from uncertainties in the target thickness measurements and in the beam integration. As a further check on the absolute cross sections, elastic scattering cross sections were measured at 36 MeV and compared with previously published data.[11] The cross sections agreed to within the accuracy ($\pm 20\%$) that the earlier data could be extracted from the published figures.

The ^{7}Li and ^{7}Be ejectiles were momentum analyzed and identified by an Enge spectrometer containing a heavy-ion gas counter in its focal plane. The total energy, differential energy loss, and position signals from the detector

made it possible to determine the mass and charge of the ejectiles. The solid angle subtended by the spectrometer was 0.75 msr and its angular acceptance was 1° in the reaction plane, except for the largest two angles where it was 2°. A solid state detector was used to monitor the target condition and beam integration during the angular distribution runs.

A typical energy spectrum for the $^{16}O(^{7}Li,^{7}Be)^{16}N$ reaction is shown in Fig. 1. The experimental energy resolution was about 70 keV. The method of determining the energy of the labeled peaks is presented in detail in an earlier work[12] that determined the ^{18}N ground state mass by the $^{18}O(^{7}Li,^{7}Be)^{18}N$ reaction. The first excited state of ^{7}Be at 0.43 MeV is also observed in the present study and the location of the peaks arising from this state are indicated in the spectrum. As can be seen from Fig. 1, the ($^{7}Li,^{7}Be$) reaction on ^{16}O selectively excites states in ^{16}N. It might be expected, because of the large angular momentum mismatch ($\sim 4\hbar$) of this reaction, that the selectivity is merely a result of the low density of high spin states. However, a known 3^+ state at 5.52 MeV and a proposed 5^+ state at 5.73 MeV are only weakly excited relative to the proposed 4^- 6.17 MeV state. The selectivity observed in the quadruplet of ground and first three excited states is the same as that for the $^{16}O(t,^{3}He)$ reaction[13] with the 2^- 0.0 MeV and 3^- 0.297 MeV states strongly populated, and the 0^- 0.121 MeV and 1^- 0.397 MeV states weakly populated.

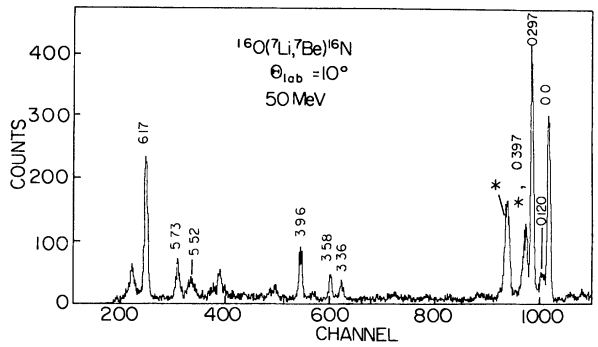

FIG. 1. A typical $^{16}O(^{7}Li,^{7}Be)^{16}N$ spectrum. Groups corresponding to the excitation of the 0.429 MeV level in ^{7}Be are marked *, and the excitation energy of states in ^{16}N are marked in MeV.

III. MICROSCOPIC THEORY OF CHARGE EXCHANGE REACTIONS

In this section the microscopic theory of direct charge exchange reactions is briefly reviewed. The charge exchange process is treated as inelastic scattering, involving changes in the spin and isospin of both the projectile and target nuclei, but not in their mass number. The form factor required for DWBA calculations may be written as

$$\langle bB \mid v \mid aA \rangle = \left\langle J_b M_b T_b M_{T_b} J_B M_B T_B M_{T_B} \left| \sum_{p,t} v_{p,t} \right| J_a M_a T_a M_{T_a} J_A M_A T_A M_{T_A} \right\rangle , \tag{1}$$

where J_x, M_x, T_x, and M_{T_x} are the spin, magnetic quantum number, isospin, and isospin projection for nucleus x. The interaction potential V is assumed to be the sum of an effective two-body nucleon-nucleon interaction $v_{p,t}$ over the nucleons in the projectile and target. The important parts of the interaction for the charge exchange reaction are the central and tensor components; in general, the spin-orbit part of the interaction produces a negligible contribution to the cross sections. The nucleon-nucleon interaction may be written in the form

$$v_{p,t}(\vec{s}) = v_{00}^0(s) + v_{01}^0(s)\vec{\tau}(p)\cdot\vec{\tau}(t) + v_{10}^0(s)\vec{\sigma}(p)\cdot\vec{\sigma}(t) + v_{11}^0(s)\vec{\sigma}(p)\cdot\vec{\sigma}(t)\vec{\tau}(p)\cdot\vec{\tau}(t) + [v_{10}^2(s) + v_{11}^2(s)\vec{\tau}(p)\cdot\vec{\tau}(t)]S_{pt} , \tag{2}$$

where $\vec{s}$ is the separation vector of the two interacting nucleons, $\vec{\sigma}$ and $\vec{\tau}$ are Pauli spin and isospin operators, and S_{pt} is the tensor operator. This may also be written in the following more compact form:

$$v_{p,t}(\vec{s}) = \sum_{\substack{K=0,2 \\ ST}} v_{ST}^K(s) C_S^K Y_K(\hat{s}) \cdot [\bar{\sigma}^S(p) \otimes \bar{\sigma}^S(t)]^K \bar{\tau}^T(p) \cdot \bar{\tau}^T(t) , \tag{3}$$

where $K=0$ corresponds to the central force, $K=2$ to the tensor force, and S,T to the spin and isospin labels of the force. The constants C_S^K have the values $C_0^0=(4\pi)^{1/2}$, $C_1^0=-(12\pi)^{1/2}$, $C_0^2=0$, and $C_1^2=(24\pi/5)^{1/2}$. When $S=0$, $\bar{\sigma}^S$ is the unit operator, and when $S=1$, it becomes the Pauli spin operator $\bar{\sigma}$. Likewise for the isospin operator $\bar{\tau}^T$.

Using the techniques of Ref. 14, the matrix element of Eq. (1) may be readily evaluated as

$$\langle bB \mid v \mid aA \rangle = \sum_{\substack{J_R M_R \\ J_p M_p \\ J_t M_t}} i^{-J_r} (-)^{J_b - M_b} \hat{J}_b \langle J_A J_t M_A M_t \mid J_B M_B \rangle \langle J_a J_b M_a, -M_b \mid J_p M_p \rangle \langle J_R J_p M_R M_p \mid J_t M_t \rangle$$

$$\times F_{M_R}^{J_R J_p J_t}(R) Y_{J_R M_R}^*(\hat{R}) , \tag{4}$$

where the radial form factor is

$$F_{M_R}^{J_R J_p J_t}(R)=\sum_{\substack{L_R L_p L_t \\ STM_T \\ K}}(4\pi)^{-1/2}(-)^{J_a-J_b+J_p+L_t+S+M_T-K}\hat{L}_p\hat{L}_t\hat{S}\,\hat{L}_R\hat{J}_R\langle L_pL_t00\,|\,L_R0\rangle\langle J_RL_R00\,|\,K0\rangle\begin{Bmatrix}L_p & S & J_p\\ L_t & S & J_t\\ L_R & K & J_R\end{Bmatrix}$$

$$\times C_K\frac{1}{2\pi^2}\int_0^\infty v_{ST}^K(k)F_{ba}^{L_pSJ_p,TM_T}(k)F_{BA}^{L_tSJ_t,TM_t}(k)j_{J_R}(kR)k^2dk\ . \tag{5}$$

In this expression J_p, J_t, and J_R represent the total angular momentum transfer to the projectile, target, and relative motion. They are equivalent to s, j, and l in the notation of Satchler.[15] Similarly, L_p, L_t, and L_R represent the orbital angular momentum transfer to the projectile, target, and relative motion. The constant C_K has the values $C_0=1$ and $C_2=2^{1/2}$. The Fourier transform of the interaction is given by

$$v_{ST}^K(k)=4\pi\int_0^\infty v_{ST}^K(s)j_K(ks)s^2ds\ , \tag{6}$$

and of the densities by

$$F_{fi}^{LSJ,TM_T}(k)=4\pi\int_0^\infty F_{fi}^{LSJ,TM_T}(r)j_L(kr)r^2dr\ . \tag{7}$$

The radial densities have the form

$$F_{fi}^{LSJ,TM_T}(r)=\sum_{j_fj_i}S_{TM_T}^J(j_fj_i)\langle l_fj_f||T^{LSJ}||l_ij_i\rangle u_{n_fl_fj_f(r)}u_{n_il_ij_i(r)}\ , \tag{8}$$

where the tensor $T_{M_J}^{LSJ}$ is formed from coupling $Y_{LM_L}(\hat{r})$ with $\bar{\sigma}^S$,

$$T_{M_J}^{LSJ}=\sum_{M_LM_S}\langle LSM_LM_S\,|\,JM_J\rangle i^LY_{LM_L}(\hat{r})\bar{\sigma}_{M_S}^S\ , \tag{9}$$

with single-particle matrix elements tabulated by Bell and Satchler.[16] The spectroscopic amplitudes $S_{TM_T}^J(j_fj_i)$ are defined by

$$S_{TM_T}^J(j_fj_i)=\frac{2^{1/2}\hat{j}_f}{\hat{J}}\langle f||A_{TM_T}^J||i\rangle\ , \tag{10}$$

where

$$A_{TM_T}^{JM_J}(j_fj_i)=\sum_{\substack{m_fm_i\\ t_{z_f}t_{z_i}}}(-)^{j_i-m_i+1/2-t_{z_i}}\langle j_fj_im_f,-m_i\,|\,JM_J\rangle\langle\tfrac{1}{2}\tfrac{1}{2}t_{z_f},-t_{z_i}\,|\,TM_T\rangle a_{j_fm_ft_{z_f}}^\dagger a_{j_im_it_{z_i}}\ . \tag{11}$$

The matrix elements in Eqs. (8) and (10) are reduced with respect to spin in the convention of Brink and Satchler.[17] The spectroscopic amplitudes have the value of unity for pure single-particle transitions and $2^{1/2}\hat{j}_f/\hat{J}$ for pure particle-hole transitions.

In the absence of spin-orbit potentials, the DWBA transition amplitude is

$$T=\int\chi_f^{(-)*}(\vec{k}_b,\vec{r})\langle bB\,|\,v\,|\,aA\rangle\chi_i^{(+)}(\vec{k}_a,\vec{r})d\vec{r}\ . \tag{12}$$

The distorted waves are expanded in partial wave series

$$\chi_i^{(+)}(\vec{k}_a,\vec{r})=\frac{4\pi}{k_ar}\sum_{L_aM_a}i^{L_a}\chi_{L_a}(k_a,r)Y_{L_aM_a}(\hat{r})Y_{L_aM_a}^*(\hat{k}_a)\ , \tag{13a}$$

$$\chi_f^{(-)*}(\vec{k}_b,\vec{r})=\frac{4\pi}{k_br}\sum_{L_bM_b}i^{-L_b}\chi_{L_b}(k_b,r)Y_{L_bM_b}^*(\hat{r})Y_{L_bM_b}(\hat{k}_b)\ . \tag{13b}$$

Using the multipole decomposition of Eq. (4) and some angular momentum algebra, the transition amplitude becomes

$$T=\frac{4\pi}{k_bk_a}(-)^{J_b-M_b}\hat{J}_b\sum_{\substack{J_RJ_pJ_t\\ M_R}}\hat{J}_R\langle J_AJ_tM_A,M_B-M_A\,|\,J_BM_B\rangle$$

$$\times\langle J_RJ_pM_R,M_a-M_b\,|\,J_tM_B-M_A\rangle\langle J_aJ_bM_a,-M_b\,|\,J_p,M_a-M_b\rangle S_{J_RJ_pJ_t}^{M_R}(\theta)\ , \tag{14}$$

where

$$S^{M_R}_{J_R J_p J_t}(\theta)=\sum_{L_a L_b} i^{L_a-L_b-J_R}(2L_b+1)(4\pi)^{-1/2}\langle L_b J_R 00\,|\,L_a 0\rangle\langle L_b J_R M_R,-M_R\,|\,L_a 0\rangle\left[\frac{(L_b-M_R)!}{(L_b+M_R)!}\right]^{1/2} P^{M_R}_{L_b}(\theta)$$

$$\times\int_0^\infty dr\,\chi_{L_b}(k_b,r)F^{J_R J_p J_t}_{M_R}(r)\chi_{L_a}(k_a,r)\,. \tag{15}$$

The differential cross section is

$$\frac{d\sigma}{d\Omega}=\frac{ab}{(2\pi\hbar^2)^2}\frac{k_b}{k_a}\frac{1}{(2J_a+1)(2J_A+1)}\sum_{\substack{M_A M_B\\ M_a M_b}}|T|^2\,, \tag{16a}$$

$$=\frac{1}{E_a E_b}\frac{k_b}{k_a}\frac{(2J_b+1)(2J_B+1)}{(2J_a+1)(2J_A+1)}$$

$$\times\sum_{\substack{J_R J_p J_t\\ M_R}}|S^{M_A}_{J_R J_p J_t}(\theta)|^2\,, \tag{16b}$$

and is thus an incoherent sum of partial cross sections corresponding to the allowed $J_R J_p J_t$ values.

IV. DATA ANALYSIS

A. Elastic scattering

In order to obtain optical potential parameters to generate distorted waves for the DWBA analysis, the elastic scattering of ^{7}Li + ^{16}O was measured at 50 MeV concurrently with the charge exchange data. The elastic scattering data is shown in Fig. 2 and was analyzed with the optical model using Woods-Saxon potentials. Starting parameters were taken from Schumacher *et al.*[11] for ^{7}Li + ^{16}O at 36 MeV, and were varied to obtain the best fit to the 50 MeV data. The resulting potential parameters are given in Table I and the fit to the data is shown in Fig. 2. The main difference between the 50 MeV parameters obtained here and the 36 MeV parameters of Ref. 11 is a reduction in the strength of the imaginary potential by almost a factor of 2.

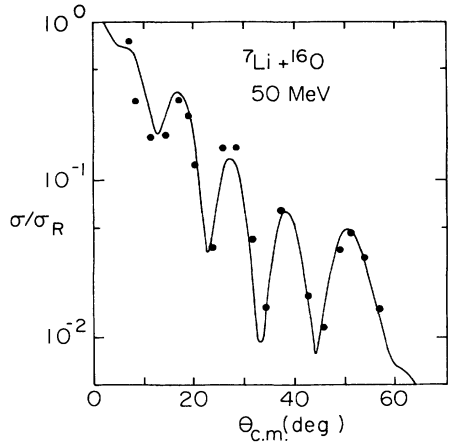

FIG. 2. ^{7}Li + ^{16}O elastic scattering data at 50 MeV fitted with the optical potential of Table I.

B. Charge exchange

The charge exchange data were analyzed in the DWBA using a microscopic form factor as described in Sec. III. The optical potential of Table I was used to generate the distorted waves in both the ^{7}Li entrance and ^{7}Be exit channels. The $T=1$ components of the nucleon-nucleon interaction are required for charge exchange reactions, and for these the effective interaction of Bertsch *et al.*[18] was employed. Single-nucleon knockout exchange was approximated for the central force by inclusion of a zero-range pseudointeraction.[19] Exchange was neglected for the tensor force since it is expected to be unimportant because of the relatively long range nature of the force. The explicit forms used for the interaction were

$$v^0_{01}(s)=-4886\frac{e^{-4s}}{4s}+1175\frac{e^{-2.5s}}{2.5s}$$

$$+310\delta(\vec{s})\,, \tag{17a}$$

$$v^0_{11}(s)=-421\frac{e^{-4s}}{4s}+480\frac{e^{-2.5s}}{2.5s}$$

$$+3.5\frac{e^{-0.7s}}{0.7s}-145\delta(\vec{s})\,, \tag{17b}$$

$$v^2_{11}(s)=386s^2\frac{e^{-2.5s}}{2.5s}+10.5s^2\frac{e^{-1.429s}}{1.429s}\,. \tag{17c}$$

The transition density for ^{7}Li$\rightarrow$^{7}Be was taken from Ref. 14 where an LS coupling model was assumed. The spectroscopic amplitudes are tabulated in Table II for transitions to the $\frac{3}{2}^-$ ground state and $\frac{1}{2}^-$ 0.43 MeV first excited state of ^{7}Be. These spectroscopic amplitudes were calculated from the proton-neutron Z^J coefficients of Ref. 20, which are related by

$$S^J_{1-1}(j_f j_i)=\frac{2^{1/2}\hat{j}_f\hat{J}_i}{\hat{J}_f}[Z^J_{\rm n}(j_f j_i)-Z^J_{\rm p}(j_f j_i)]\,. \tag{18}$$

Harmonic oscillator radial wave functions were used with $\alpha=0.578$ fm^{-1} on the basis of Refs. 15 and 20.

Transitions to three states in ^{16}N are considered here: the 2^- ground state, the 3^- 0.297 MeV state, and the 4^- 6.17 MeV state. The 2^- and 3^- states have almost pure $1d_{5/2}1p^{-1}_{1/2}$ configurations, while the 4^- state is the so-called "stretched" state with a $1d_{5/2}1p^{-1}_{3/2}$ configuration. The shell model calculations of Picklesimer and Walker, as described in Ref. 21, were used for these states. The spectroscopic amplitudes are given in Table III. Again harmonic oscillator radial wave functions were used with $\alpha=0.580$ fm^{-1} to obtain an rms charge radius of 2.71 fm in agreement with measured values.[22]

For each transition three DWBA calculations were

TABLE I. Optical potential parameters for ^{7}Li + ^{16}O at 50 MeV.

V (MeV)	r_R [a] (fm)	a_R (fm)	W (MeV)	r_I [a] (fm)	a_I (fm)	r_c [a] (fm)
170.3	1.21	0.777	11.38	2.101	0.951	1.3

[a] $R_x = r_x A_T^{1/3}$.

made: with the total interaction ($C+T$), with only the central part of the interaction (C), and with only the tensor part (T). The results of the calculations are shown as the full, dot-dashed, and dashed curves in Fig. 3. The excitation of the 2^- ground state of ^{16}N is an unnatural parity transition and thus proceeds only through the $S=1$ part of the interaction. The central force alone produces an angular distribution which has too much oscillatory structure compared with the data, whereas the angular distribution from the tensor force is much more structureless and larger in magnitude. The total calculation reproduces the shape of the data reasonably, although the calculated cross sections must be multiplied by 2.2 to obtain the correct magnitude. There are two experimental angular distributions for excitation of the 3^- 0.297 MeV state where the ^{7}Be is either in its ground state (^{7}Be$_0$) or first excited state (^{7}Be$_1$). This is a natural parity transition and for ^{7}Be$_0$ has a contribution from the $S=0$ central force in addition to the $S=1$ central and tensor forces. For both the ^{7}Be$_0$ and ^{7}Be$_1$ cases, the shape of the data is reproduced reasonably and is dominated by the central force, the tensor contributions being an order of magnitude or more smaller. However, the calculations must be multiplied by 8.5 and 5.1, respectively. Excitation of the 4^- 6.17 MeV stretched state is again an unnatural parity transition with the tensor force dominating. Both the angular distributions calculated with the central and tensor forces only have a similar shape to the data, with the cross sections from the tensor force alone being about six times larger than with the central force alone. The total calculated cross section needs to be multiplied by 6.5 to obtain the correct magnitude.

V. DISCUSSION AND CONCLUSIONS

In the previous section we have found that our microscopic analysis of the (^{7}Li,^{7}Be) reaction resulted in cross sections which underestimated the measured cross sections by factors of 2.2 to 8.5. This is now discussed, for the cases where the ^{7}Be nucleus is emitted in its ground state, with reference to inelastic electron, proton, and pion scattering and other charge exchange measurements.

Inelastic electron scattering to the analogs of the ^{16}N 2^- ground and 3^- 0.297 MeV states in ^{16}O has been measured by Sick *et al.*[8] The two states were unresolved and the data also contained an unresolved 1^- $2s_{1/2}1p_{1/2}^{-1}$ contribution. When particle-hole wave functions were assumed, the calculated electron scattering form factors had to be multiplied by 0.59 to fit the measurements. Fazely *et al.*[21] have made microscopic distorted-wave impulse approximation (DWIA) calculations of the ^{16}O(p,n)^{16}F reaction to the 2^- 0.4 MeV and 3^- 0.7 MeV states in ^{16}F. These are the analogs in ^{16}F of the 2^- and 3^- states we have observed in ^{16}N. Their calculations made use of the Love and Franey[23] effective interaction and the same shell model wave functions we have used. The two states were unresolved, but the shapes of the data and the calculations showed that the forward angles were dominated by the 2^- state and the larger angles by the 3^- state. Their calculations needed to be multiplied by 0.47 and 0.23 for the 2^- and 3^- contributions, respectively, to obtain the correct magnitude. These normalizations are consistent with the (e,e′) normalization, within the errors of the nucleon-nucleon interaction, and indicate that since the (e,e′) reaction only populates, in a single step, 1p1h states based on the ^{16}O ground state, the (p,n) reaction also populates 1p1h configurations with relatively small multistep contributions. The ^{16}O(n,p)^{16}N reaction has been measured[24] at 60 MeV and a proton group was observed for an excitation of 0.2 MeV in ^{16}N. The data were consistent with a 2^- state having a $J_R=1$ character. In the ^{16}O(^{7}Li,^{7}Be)^{16}N measurements reported here we were able to resolve the 2^- and 3^- states in ^{16}N. For the 2^- state the $J_R J_p J_t = 112$ and 312 contributions have similar magnitudes near 0° and 30°–60°, but the 312 contribution follows the shape of the data well, whereas the 112 contribution has a deep minimum near 12° which is not present in the data. The $J_R J_p J_t = 303$ and 313 contributions for the 3^- state have very similar shapes and magnitudes. In contrast to the (e,e′) and (p,n) results which need a *reduction* in the calculated cross sections, our calculated cross sections for (^{7}Li,^{7}Be) need to be *increased* by 2.2 or 8.5.

TABLE II. Spectroscopic amplitudes $S^J_{1-1}(j_f j_i)$ for ^{7}Li→^{7}Be.

Transition	J	$1p_{3/2}$ $1p_{3/2}^{-1}$	$1p_{1/2}$ $1p_{1/2}^{-1}$	$1p_{3/2}$ $1p_{1/2}^{-1}$	$1p_{1/2}$ $1p_{3/2}^{-1}$
$\frac{3}{2}^- \rightarrow \frac{3}{2}^-$	0	0.786	0.629	0	0
	1	−0.325	0.373	0.515	−0.363
	2	−0.031	0	0.438	−0.310
	3	−0.849	0	0	0
$\frac{3}{2}^- \rightarrow \frac{1}{2}^-$	1	0.728	0.147	−0.295	0.680
	2	0.619	0	0.892	0.221

TABLE III. Spectroscopic amplitudes $S^{J}_{11}(j_f j_i)$ for $^{16}O \rightarrow {}^{16}N$.

Transition	J	$1d_{3/2}$ $1p^{-1}_{3/2}$	$1d_{5/2}$ $1p^{-1}_{1/2}$	$1d_{5/2}$ $1p^{-1}_{3/2}$	$1d_{3/2}$ $1p^{-1}_{1/2}$	$2s_{1/2}$ $1p^{-1}_{3/2}$
$0^+ \rightarrow 2^-$	2	0.087	1.515	0.286	−0.028	0.057
$0^+ \rightarrow 3^-$	3	0.007	1.294	−0.199	0	0
$0^+ \rightarrow 4^-$	4	0	0	1.155	0	0

This indicates, if we assume that the 1p1h wave function of these states has been determined by the (e,e′) and (p,n) measurements, that either the effective interaction or reaction mechanism (or both) that we have used is incorrect.

The analog of the 4^- stretched state in ^{16}O has been investigated by the inelastic scattering of protons,[6,21] pions,[7] and electrons.[8] Assuming a pure $d_{5/2}p^{-1}_{3/2}$ configuration and harmonic oscillator single particle wave functions, only 44% of the one-body $T=1$ strength was observed in the (e,e′) results. The (p,p′) and (π,π') measurements were reproduced with only a small additional normalization compared to the (e,e′) results. The measured[21] cross sections for $^{16}O(p,n)^{16}F(4^-)$ have a $J_R=3$ character and are described well by microscopic DWIA calculations if these are multiplied by 0.31. This normalization is consistent with the inelastic scattering measurements and supports the single-step nature of the (p,n) reaction. A $J_R=3$ transition for an excitation energy of 6.2 MeV in ^{16}N is observed[24] in the $^{16}O(n,p)^{16}N$ reaction. Our calculations for $^{16}O(^{7}Li,^{7}Be)^{16}N(4^-)$ indicate that the

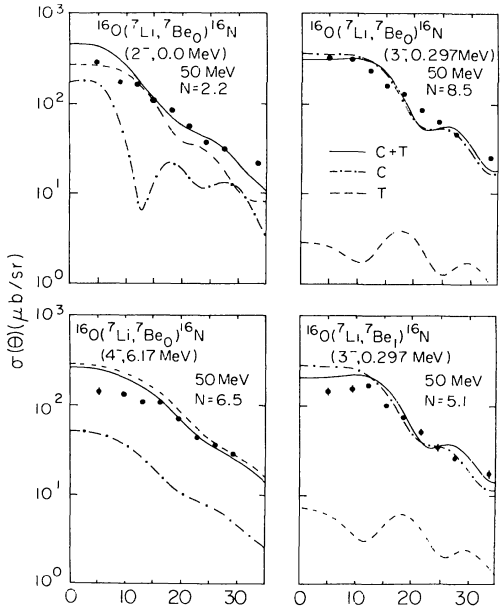

FIG. 3. $^{16}O(^{7}Li,^{7}Be)^{16}N$ charge exchange data at 50 MeV compared with microscopic DWBA calculations. $^{7}Be_0$ and $^{7}Be_1$ correspond to the ejectile in the $\frac{3}{2}^-$ ground and $\frac{1}{2}^-$ 0.43 MeV first excited states. The full curve corresponds to a central and tensor ($C+T$) interaction, while the dot-dashed and dashed curves are the angular distributions obtained from a central (C) and tensor (T) interaction alone. The calculated cross sections have been multiplied by the factor N.

$J_R J_p J_t = 314$ and 514 contributions have very similar shapes, with the 314 contribution being about twice as large in magnitude. The calculated cross section for ($^{7}Li,^{7}Be$) needs to be *increased* by a factor of 6.5 to fit the data, and again indicates a deficiency in our model.

Williams-Norton *et al.*[2] have made microscopic calculations of the $^{40}Ca(^{7}Li,^{7}Be)^{40}K$ reaction employing the same central interaction we have used here, but omitting the tensor part. We have repeated their calculations and found that their results are 4π times too large. The calculated cross sections then need to be multiplied by factors of 25—75 to fit the experimental data. These results, together with those for $^{16}O(^{7}Li,^{7}Be)^{16}N$ reported here, show that there is a wide discrepancy between simple single-step microscopic calculations and measured cross sections, which may include some mass dependence.

There are three aspects to be considered in the microscopic treatment of heavy-ion reactions: (1) the structure of the projectile and target, (2) the effective interaction, and (3) the reaction mechanism. These three are inextricably interwoven and thus it may not be possible to determine one without knowledge of the other two, which also depend on the first aspect considered. In our treatment of the $^{16}O(^{7}Li,^{7}Be)^{16}N$ reaction we have used transition densities which are consistent with (e,e′), (p,p′), and (p,n) measurements. These, of course, make assumptions about the underlying interactions and reaction mechanisms. However, since the interaction is known in the case of (e,e′) and the transitions here are of a single-step nature, the consistency of the results from all three processes indicates that the wave functions are reasonably well determined. Any deficiencies in the wave functions, such as the omission of the ~25% 2p2h component of the ^{16}O ground state, would be present in these measurements as well as in the ($^{7}Li,^{7}Be$) reaction, and thus are unlikely to be the cause of the discrepancy in normalizations.

The calculations presented here have used a purely real form factor. An imaginary part could arise from coupling to other reaction channels or due to an imaginary part of the underlying nucleon-nucleon interaction. The elastic and inelastic scattering of ^{7}Li is often dominated by the imaginary part of the optical potential or transition form factor, which are treated phenomenologically. Two-step contributions, particularly the ($^{7}Li,^{6}Li$)($^{6}Li,^{7}Be$) mechanism, could be important for the ($^{7}Li,^{7}Be$) charge exchange reaction and could possibly be accounted for by an imaginary form factor. These processes may also have a real part. The effective nucleon-nucleon interaction is expected[25] to be complex, and the contribution of the imaginary part for natural parity transitions has been simulated[26] by an imaginary collective model. The imaginary part of $v^0_{01}(s)$ could alter our conclusions about the

3^- 0.297 MeV state in ^{16}N, but would not change our overall conclusions since it does not contribute to excitation of the 2^- and 4^- states. The relevant $S=1$ $T=1$ components of the nucleon-nucleon force for excitation of these states are known[27] to be nearly real and thus the omission of an imaginary part here is not considered to be significant.

Finally, we come to the problem of the reaction mechanism. We had assumed throughout this paper a single-step mechanism for the (^{7}Li,^{7}Be) reaction. Multistep contributions may also be important, particularly the (^{7}Li,^{6}Li)(^{6}Li,^{7}Be) path. Inclusion of this path [in a two-step DWBA or coupled-reaction channel (CRC) calculation] would require knowledge of the ^{16}O(^{7}Li,^{6}Li)^{17}O and ^{17}O(^{6}Li,^{7}Be)^{16}N reactions. However, to make microscopic calculations of these we would also have the difficulty of determining the correct wave functions, interaction, and reaction mechanism. The problem is therefore not solved by adopting this hypothesis, particularly since there is no experimental signature in the cross sections as to whether a reaction is one-step or multistep.

In conclusion, we report measurements of the ^{16}O(^{7}Li,^{7}Be)^{16}N reaction at 50 MeV to selectively populated $T=1$ states in ^{16}N. Microscopic DWBA calculations, including the tensor part of the interaction which is important for the unnatural parity states, are able to reproduce the shapes of the angular distributions, but underestimate the magnitudes of the cross sections by factors of 1.6—8.5.

ACKNOWLEDGMENTS

The authors acknowledge helpful discussions with Dr. F. Petrovich. This work was supported in part by the National Science Foundation.

[1]M. E. Williams-Norton, F. Petrovich, K. W. Kemper, G. M. Hudson, R. J. Puigh, and A. F. Zeller, Nucl. Phys. **275**, 509 (1977).

[2]M. E. Williams-Norton, F. Petrovich, K. W. Kemper, R. J. Puigh, D. Stanley, and A. F. Zeller, Nucl. Phys. **A313**, 477 (1979).

[3]V. Gillet and N. Vinh-Mau, Nucl. Phys. **54**, 321 (1964).

[4]G. Mairle, G. J. Wagner, P. Doll, K. T. Knöpfle, and H. Breuer, Nucl. Phys. **A299**, 39 (1978).

[5]D. J. Millener and D. Kurath, Nucl. Phys. **A255**, 315 (1975).

[6]R. S. Henderson, B. M. Spicer, I. D. Svalbe, V. C. Officer, G. G. Shute, D. W. Devins, D. L. Friesel, W. P. Jones, and A. C. Attard, Aust. J. Phys. **32**, 411 (1979).

[7]D. B. Holtkamp, W. J. Braithwaite, W. Cottingame, S. J. Greene, R. J. Joseph, C. F. Moore, C. L. Morris, J. Piffaretti, E. R. Siciliano, H. A. Thiessen, and D. Dehnhard, Phys. Rev. Lett. **45**, 420 (1980).

[8]I. Sick, E. B. Hughes, T. W. Donnelly, J. D. Walecka, and G. E. Walker, Phys. Rev. Lett. **23**, 1117 (1969); W. Bertozzi, Nucl. Phys. **A374**, 109c (1982).

[9]K. W. Kemper, G. G. Shute, C. H. Atwood, L. K. Fifield, and T. R. Ophel, Nucl. Phys. **A405**, 348 (1983).

[10]V. Gomes, R. A. Douglas, T. Polga, and O. Sala, Nucl. Phys. **68**, 417 (1965).

[11]P. Schumacher, N. Ueta, H. H. Duhm, K.-I. Kubo, and W. J. Klages, Nucl. Phys. **A212**, 573 (1973).

[12]G. P. Putt, L. K. Fifield, M. A. G. Hotchkis, T. R. Ophel, and D. C. Weisser, Nucl. Phys. **A399**, 190 (1983).

[13]E. R. Flynn and J. D. Garrett, Phys. Rev. C **10**, 409 (1974).

[14]F. Petrovich and D. Stanley, Nucl. Phys. **A275**, 487 (1977).

[15]G. R. Satchler, Nucl. Phys. **55**, 1 (1964).

[16]W. K. Bell and G. R. Satchler, Nucl. Data Tables **A9**, 147 (1971).

[17]D. M. Brink and G. R. Satchler, *Angular Momentum* (Oxford University, New York, 1968).

[18]G. Bertsch, J. Borysowicz, H. McManus, and W. G. Love, Nucl. Phys. **A284**, 399 (1977).

[19]M. Golin, F. Petrovich, and D. Robson, Phys. Lett. **64B**, 253 (1976).

[20]F. Petrovich, R. H. Howell, C. H. Poppe, S. M. Austin, and G. M. Crawley, Nucl. Phys. **A383**, 355 (1982).

[21]A. Fazely, B. D. Anderson, M. Ahmad, A. R. Baldwin, A. M. Kalenda, R. J. McCarthy, J. W. Watson, R. Madey, W. Bertozzi, T. N. Buti, J. M. Finn, M. A. Kovash, B. Pugh, and C. C. Foster, Phys. Rev. C **25**, 1760 (1982).

[22]C. W. de Jager, H. de Vries, and C. de Vries, At. Data Nucl. Data Tables **14**, 479 (1974).

[23]W. G. Love and M. A. Franey, Phys. Rev. C **24**, 1073 (1981).

[24]G. A. Needham, F. P. Brady, D. H. Fitzgerald, J. L. Romero, J. L. Ulmann, J. W. Watson, C. Zanelli, N. S. P. King, and G. R. Satchler, Nucl. Phys. **A385**, 349 (1982).

[25]*Lecture Notes in Physics 89, Microscopic Optical Potentials,* edited by H. V. von Geramb (Springer, New York, 1979).

[26]G. R. Satchler, Phys. Lett. **35B**, 279 (1971).

[27]M. R. Anastasio and G. E. Brown, Nucl. Phys. **A285**, 516 (1977); S. Yen, R. J. Sobie, T. E. Drake, A. D. Bacher, G. T. Emery, W. P. Jones, D. Miller, C. Olmer, P. Schwandt, W. G. Love, and F. Petrovich, Phys. Lett. **105B**, 421 (1981).